Figure S1

A

Screen	# of worms screened	# of viable RNAi(+) mutants	# of RNAe mutants
F1	1M	0	0
F2	1M	1	0
F3	1M	292	34
F4	2M	375	23
control (without ENU)	1M	0 viable	

B

nrde-1
nrde-2
nrde-4

wago-1
wago-9/hrde-1

hpl-2
mes-2
mes-3
mes-4
mes-6
set-25
set-32

C

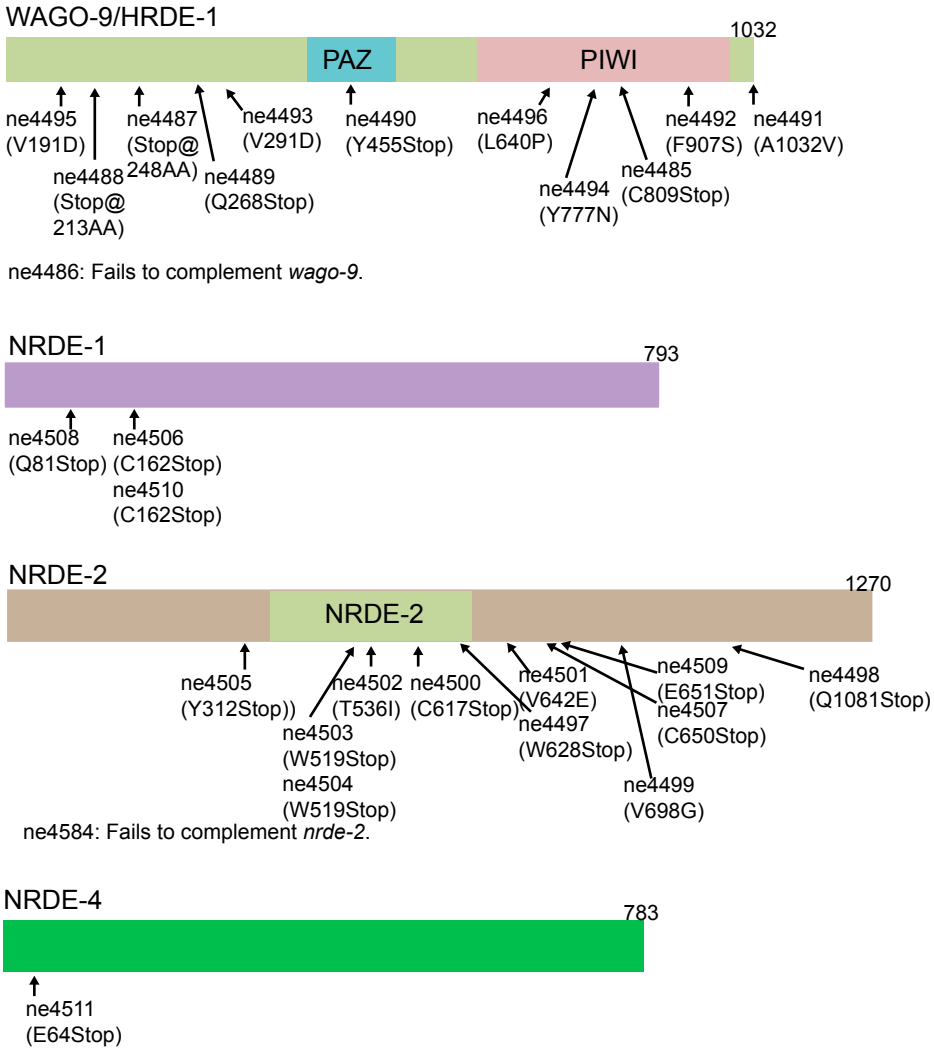

Figure S1. Detail of the screen. Related to Figure 1.
(A) Table summarizing the screen. M indicates million.
(B) List of candidate genes subjected to bulk targeted sequencing approach using the PCR-amplicon library.
(C) Schematic diagram depicting the architecture of predicted domains as well as the positions and the nature of the mutations of isolated mutants indicated.

Figure S2

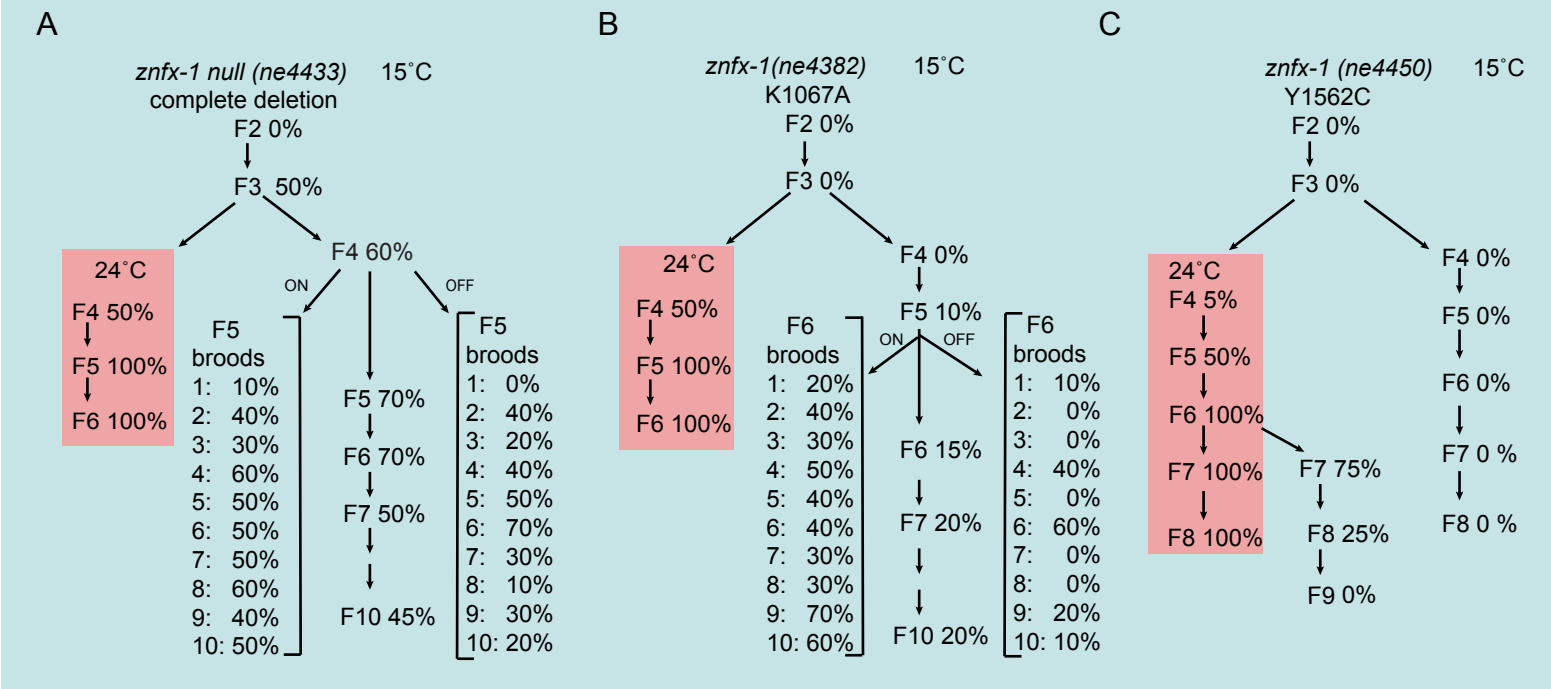

Figure S2. Temperature dependence of RNAe defect of znfx-1 mutants. Related to Figure 2.
(A-C) Schematic diagram depicting the expression states of *cdk-1::gfp* transgene across generations following the CRISPR induction of complete deletion of *znfx-1* (A), of K1067A mutation (B) or of Y1562C mutation (C) in the starting strain, at 24˚C (light red background) and 15˚C (light blue background). At each generation ~100 L1 larvae were transferred to fresh plate and 10 hermaphrodites were randomly picked and scored for *cdk-1::gfp* expression. Ten animals from the F4 generation (complete deletion) or F5 generation (K1067A) that scored ON or OFF at 15˚C were individually recovered from the slides, and *cdk-1::gfp* expression states were scored in the next generation.

Figure S3

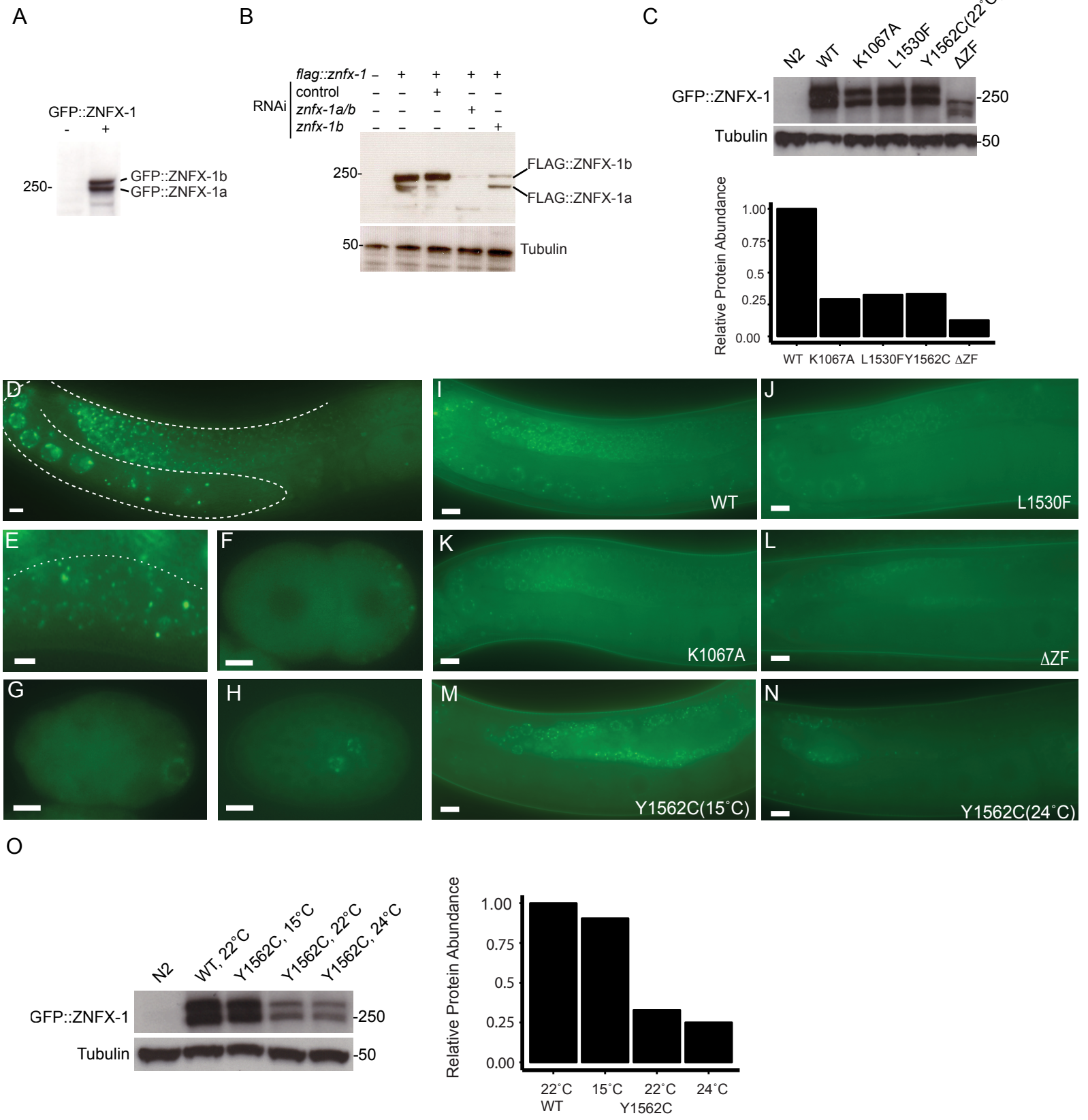

Figure S3. Expression and localization of wild-type ZNFX-1 protein and mutant proteins harboring various mutations. Related to Figure 2.
(A) Western blot using α-GFP antibody, analyzing the expression of GFP::ZNFX-1 protein.
(B) Western blot using α-flag antibody, analyzing the expression of 3Xflag::ZNFX-1 proteins in the lysate prepared from animals exposed to indicated RNAi food as described in Figure 2A.
(C) Western blot using α-GFP antibody, analyzing the expression of GFP::ZNFX-1 proteins harboring indicated mutations. Lower panel indicates relative amounts of wildtype and mutant ZNFX-1 proteins after normalized to tubulin levels.
(D to H) Fluorescent micrographs indicating the localization of GFP::ZNFX-1 in germline of adult (D), L2 larvae (E), two-cell stage embryo (F), and later stage embryos (G and H). Scale bars represent 5μm.
(I to N) Fluorescent micrographs of representative germline of animals expressing indicated GFP::ZNFX-1 proteins. Scale bars represent 10μm.
(O) Western blot using α-GFP antibody, analyzing the expression levels of indicated GFP::ZNFX-1 proteins at the indicated temperatures. Right panel indicates relative protein amounts after normalized to tubulin levels.

Figure S4

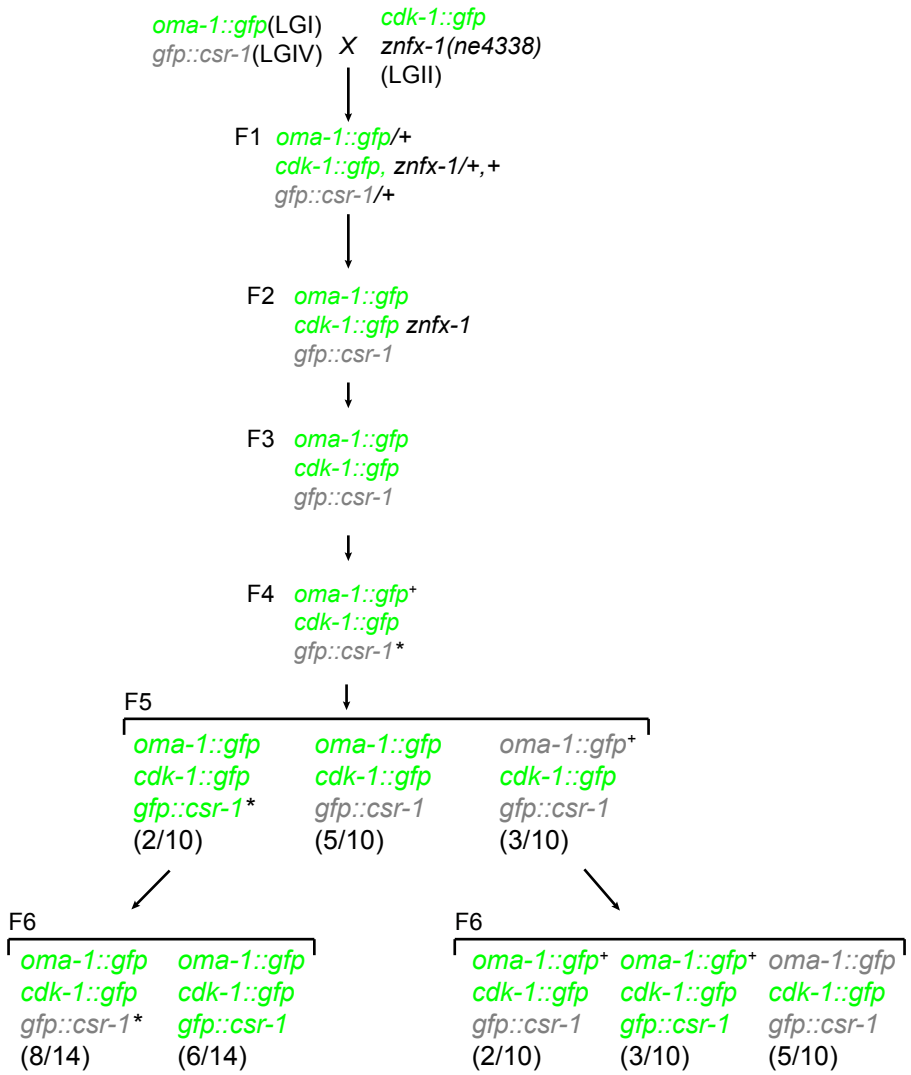

Figure S4. Variegation of transgene expression across generations. Related to Figure 4.
Schematic diagram depicting the expression states of transgenes after the cross described in Figure 4. F2 animals homozygous for all the transgenes were followed by transferring ~100 L1s to fresh plate at each generation and checking 10 randomly picked young adult hermaphrodites for GFP expression. Green color represents expressed transgene while gray represents non-expressed transgene. The transgene expression variegated in F5 and each scored animals were individually recovered and checked again in F6 for vaiegation across generation. For example, ON *oma-1::gfp* transgene in F4 designated with "+" could be silenced in F5 and again expressed in F6. Likewise, OFF *gfp::csr-1* transgene in F4 designated with "*" could be expressed in F5 and again silenced in F6.

Figure S5

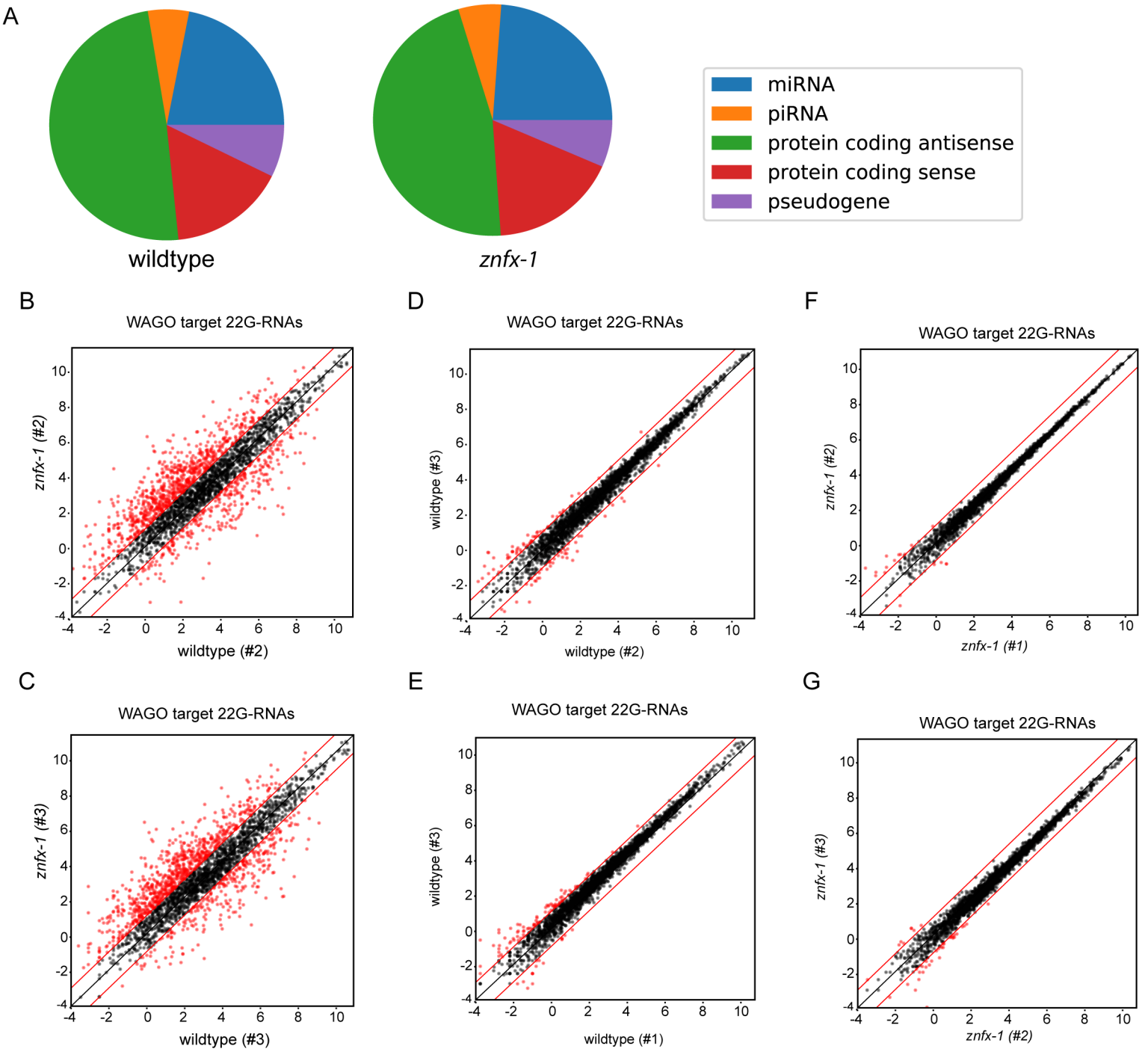

Figure S5. Small RNA profile and WAGO target 22Gs in znfx-1 mutant. Related to Figure 6.
(A) Pie charts depicting the distribution of reads that match indicated genome annotation sequenced in wildtype and *znfx-1* mutant small RNA libraries
(B and C) Scatter plots comparing the numbers of small RNA reads (log2) of WAGO targets cloned from wildtype or *znfx-1* mutant as in FIgure 6(A).
(D and E) Scatter plots as in (B and C) but comparing two independent wildtype populations.
(F and G) Scatter plots as in (B and C) but comparing two independent *znfx-1* populations.

Figure S6

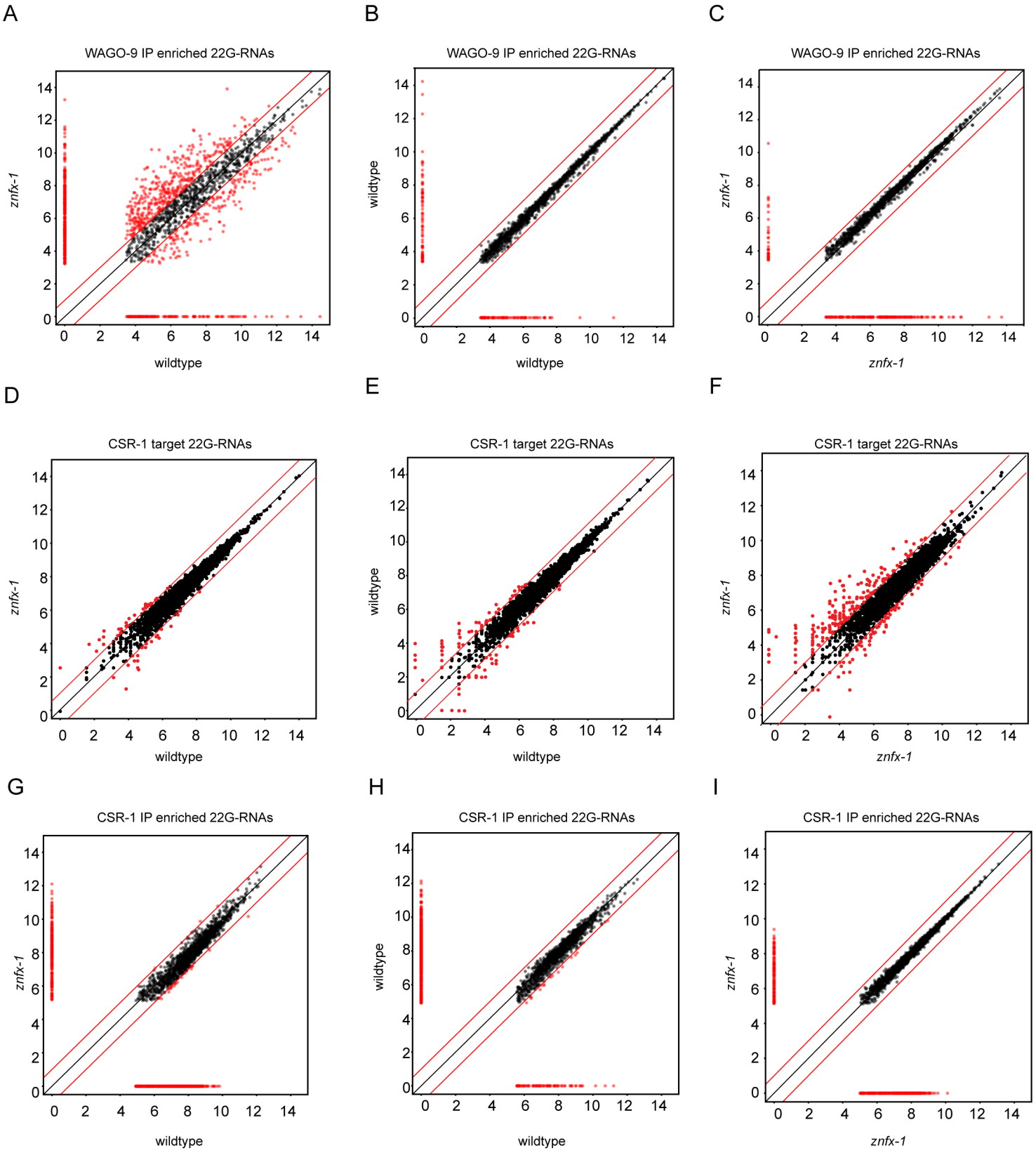

Figure S6. WAGO-9 bound 22Gs, CSR-1 target 22Gs, and CSR-1 bound 22Gs in znfx-1 mutant. Related to Figure 6.
(A to C) Scatter plots comapring the numbers of small RNA reads (log2) enriched in WAGO-9 IP from wildtype or znfx-1 mutant (A), two independent wildtype populations (B) or two independent znfx-1 populations (C). Each dot represents a gene. Dots in red represent genes with greater than 2-fold change.
(D to F) Scatter plots comparing the numbers of small RNA reads (log2) of CSR-1 targets cloned from wildtype or znfx-1 mutant (D), two independent wildtype populations (E) or two independent znfx-1 populations (F). Each dot represents a gene. Dots in red represent genes with greater than 2-fold change.
(G to I) Scatter plots comapring the numbers of small RNA reads (log2) enriched in CSR-1 IP from wildtype or znfx-1 mutant (A), two independent wildtype populations (B) or two independent znfx-1 populations (C). Each dot represents a gene. Dots in red represent genes with greater than 2-fold change.

Figure S7

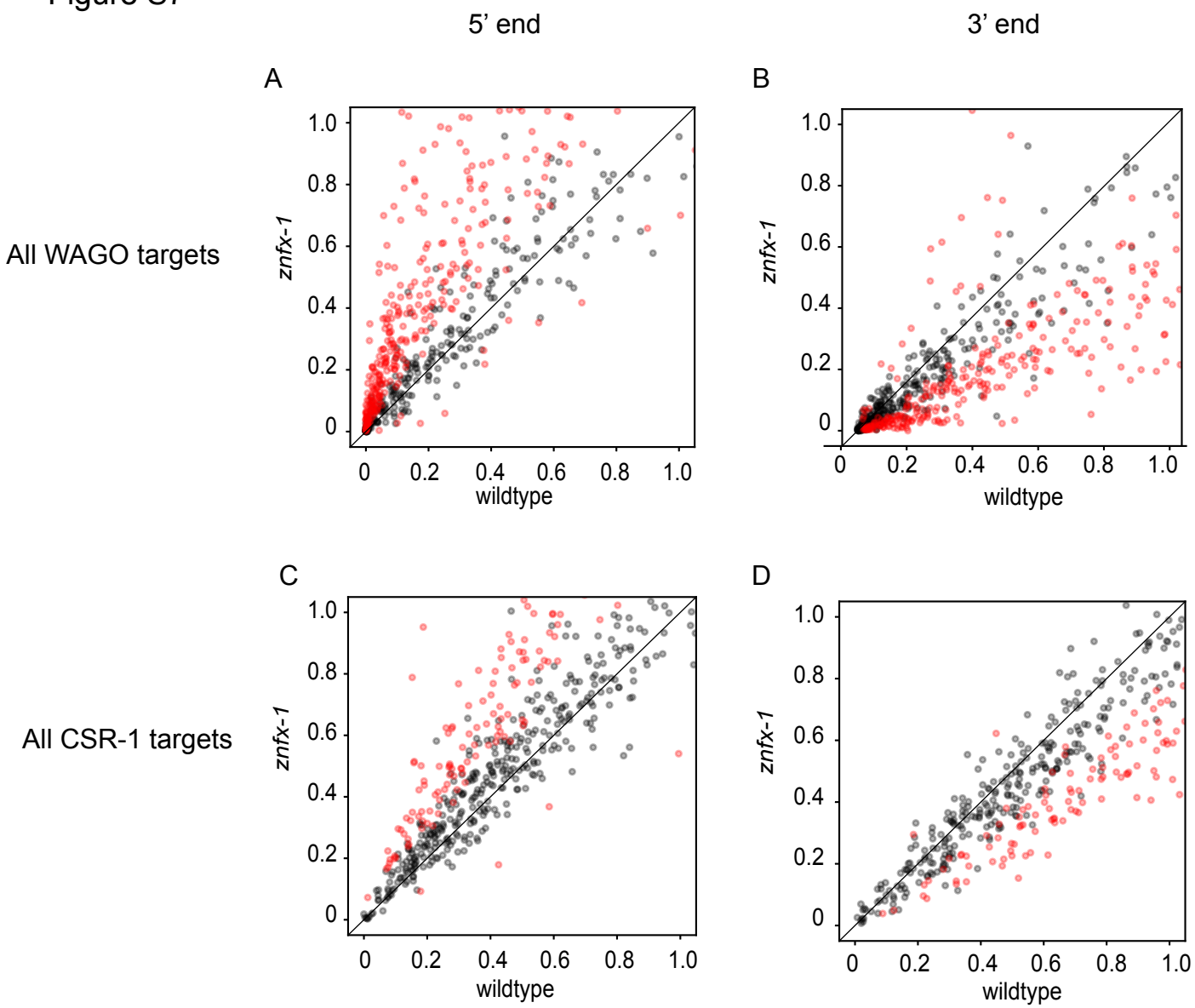

Figure S7. Scatter plots comparing 22G levels at 5’ and 3’ end of genes. Related to FIgure 6.
(A and B) Scatter plots comparing the numbers of genewise-normalized small RNA reads of WAGO targets cloned from wildtype or *znfx-1* in 6 replicates, targeting 5’ 10% (A) or 3’ 10% (B) of genes. Each dot represents a gene. Dots in red represent genes with statistically significant changes (p value < 0.05).
(C and D) Scatter plots comparing the numbers of genewise-normalized small RNA reads of CSR-1 targets cloned from wildtype or *znfx-1* in 6 replicates, targeting 5’ 10% (A) or 3’ 10% (B) of genes. Each dot represents a gene. Dots in red represent genes with statistically significant changes (p value < 0.05).

Supplementary Table 1. List of Strains. Related to Star Method.

WM296 prg-1(tm872) I; neSi11[*gfp::cdk-1*(RNAe) cb-unc-119(+)] II; unc-119(ed9) III

WM348 *csr-1*(ne4520[flag::TEV::*csr-1*]) IV

WM462 lin-11(ne832) I: neSi14[*cdk-1::gfp* (RNAe) cb-unc-119(+)] II: unc-119(ed9) cdk-1(ne2257) III: neSi10[gfp::*csr-1* (RNAe) cb-unc-119(+)] IV

WM491 lin-11(ne4519) neSi28[*oma-1::gfp* (RNAa) cb-unc-119(+)] I; neSi14[*cdk-1::gfp* cb-unc-119(+)] II; cdk-1(ne2257)III; neSi10[gfp::*csr-1*(RNAe) cb-unc-119(+)] IV

WM492 dpy-10(e128) neSi11[*gfp::cdk-1*(RNAe) cb-unc-119(+)] II: unc-119(ed9) III

WM493 dpy-10(e128) neSi8[gfp::*csr-1*(RNAe) cb-unc-119(+)] II: unc-119(ed9) III

WM494 lin-11(ne832) I: neSi14[*cdk-1::gfp,* cb-unc-119(+)] znfx-1(ne4338) II : unc-119(ed9) cdk-1(ne2257) III: neSi10[gfp::*csr-1*, cb-unc-119(+)] IV

WM495 lin-11(ne832) I: neSi14[*cdk-1::gfp,* cb-unc-119(+)] znfx-1(ne4354) II: unc-119(ed9) cdk-1(ne2257) III: neSi10[gfp::*csr-1*, cb-unc-119(+)] IV

WM496 lin-11(ne832) I: neSi14[*cdk-1::gfp,* cb-unc-119(+)] znfx-1(ne4415) II: unc-119(ed9) cdk-1(ne2257) III: neSi10[gfp::*csr-1*, cb-unc-119(+)] IV

WM497 neSi14[*cdk-1::gfp,* cb-unc-119(+)] *znfx-1*(ne4384) II: unc-119(ed9) cdk-1(ne2257) III: neSi10[gfp::*csr-1*, cb-unc-119(+)] IV

WM498 neSi14[*cdk-1::gfp*, cb-unc-119(+)] *znfx-1*(ne4381[∆zinc finger]) II: unc-119(ed9) cdk-1(ne2257) III: neSi10[gfp::*csr*-1, cb-unc-119(+)] IV

WM499 neSi14[*cdk-1::gfp*, cb-unc-119(+)] *znfx-1*(ne4399[∆helicase]) II; unc-119(ed9) cdk-1(ne2257) III: neSi10[gfp::*csr-1*, cb-unc-119(+)] IV

WM500 neSi14[*cdk-1::gfp*, cb-unc-119(+)] *znfx-1*(ne4433[complete deletion]) II: unc-119(ed9) cdk-1(ne2257) III: neSi10[gfp::*csr-1*, cb-unc-119(+)] IV

WM523 neSi14[*cdk-1::gfp*, cb-unc-119(+)] *znfx-1*(ne4449)II: unc-119(ed9) cdk-1(ne2257) III: neSi10[gfp::*csr-1,* cb-unc-119(+)] IV

WM524 neSi14[*cdk-1::gfp*, cb-unc-119(+)] *znfx-1*(ne4450) II: unc-119(ed9) cdk-1(ne2257) III: neSi10[gfp::*csr-1*, cb-unc-119(+)] IV

WM525 neSi14[*cdk-1::gfp*, cb-unc-119(+)] *znfx-1*(ne4353) II: unc-119(ed9) cdk-1(ne2257) III: neSi10[gfp::*csr-1,* cb-unc-119(+)] IV

WM501 *znfx-1*(ne4352[GFP::ZNFX-1])

WM502 *znfx-1*(ne4404[GFP::ZNFX-1[L1530F]])

WM503 *znfx-1*(ne4383[GFP::ZNFX-1[K1067A]])

WM504 *znfx-1*(ne4513[GFP::ZNFX-1[∆zinc finger]])

WM505 *znfx-1*(ne4459[GFP::ZNFX-1[Y1562C]])

WM506 *znfx-1*(ne4355[3Xflag::TEV::ZNFX-1])

WM507 *neSi14[cdk-1::gfp (RNAe) cb-unc-119(+)] znfx-1(ne4338)*

WM508 *neSi14[cdk-1::gfp (RNAe) cb-unc-119(+)] znfx-1(ne4354)*

WM509 *znfx-1(ne4352[GFP::ZNFX-1]); mCherry::pgl-1*

WM510 *znfx-1(ne4352[GFP::ZNFX-1]); csr-1(ne4515[mCherry::CSR-1]])*

WM511 *znfx-1(ne4352[GFP::ZNFX-1]); csr-1(tm892)/DnT1*

WM512 *znfx-1(ne4352[GFP::ZNFX-1]); glh-1(ok439)*

WM513 *neSi14[cdk-1::gfp (+) cb-unc-119(+)] II unc-4(ne4516) znfx-1(ne4338): unc-119(ed9) cdk-1(ne2257) III*

WM514 *ego-1(ne4518[GFP::EGO-1]) I; znfx-1(ne4355[3Xflag::TEV::ZNFX-1])II*

WM515 *znfx-1(ne4352[GFP::ZNFX-1])II; csr-1(ne4520[3Xflag::CSR-1])IV*

WM516 *znfx-1(ne4352[GFP::ZNFX-1])II; wago-9(ne4336[3Xflag::TEV::WAGO-9])III*

WM517 *wago-1(ne4585[3Xflag::TEV::SNAP::WAGO-1])I; znfx-*

	1(ne4352[GFP::ZNFX-1])II;
WM518	*znfx-1(ne4352[GFP::ZNFX-1])II; prg-1(ne4586[flag::TEV::PRG-1])*
WM519	*znfx-1(ne4354) II; csr-1(ne4520[flag::TEV::CSR-1]) IV*
WM520	*znfx-1(ne4354) II; wago-9(ne4336[flag::TEV::WAGO-9]) IV*
WM521	*wago-9(ne4336[3Xflag::TEV::WAGO-9])III*
WM522	*ego-1(ne4518[GFP::EGO-1])I*
WM603	*wago-1(ne4585[3Xflag::TEV::SNAP::WAGO-1])I*
WM604	*prg-1(ne4586[flag::TEV::PRG-1])I*
WM605	*prg-1(tm872);znfx-1(ne4338)*

Supplementary Table 2. Related to Figure 6. Distribution of reads in the small RNA libraries used in the study.

Sample	total reads	structural(%)	piRNA(%)	miRNA(%)	22G(%)
csr-1(IP)input_wt_1	14.99	8.99	3.21	8.02	12.46
csr-1(IP)input_wt_2	21.22	4.43	3.10	7.65	14.89
csr-1(IP)input_wt_3	18.07	6.21	3.36	6.14	15.78
wago-9(IP)input_wt_1	24.66	5.19	3.03	9.47	12.31
wago-9(IP)input_wt_2	15.93	8.21	3.17	7.72	13.38
wago-9(IP)input_wt_3	18.97	12.38	2.88	6.98	12.68
csr-1(IP)input_znfx-1_1	17.10	5.39	3.37	8.30	13.49
csr-1(IP)input_znfx-1_2	18.89	3.93	3.58	7.37	15.27
csr-1(IP)input_znfx-1_3	24.10	7.17	3.54	6.31	14.90
wago-9(IP)input_znfx-1_1	21.10	8.24	3.23	7.79	14.62
wago-9(IP)input_znfx-1_2	19.74	4.75	2.45	8.15	16.38
wago-9(IP)input_znfx-1_3	19.52	5.99	3.62	5.54	17.98
csr1(IP)_wt_1	23.52	11.26	6.66	1.86	11.58
csr-1(IP)_wt_2	21.62	5.91	1.08	1.58	13.78
csr-1(IP)_wt_3	10.50	4.68	0.61	0.92	15.24
csr-1(IP)_znfx-1_1	26.84	9.79	8.09	2.22	11.33
csr-1(IP)_znfx-1_2	12.71	4.25	0.44	1.15	15.37
csr-1(IP)_znfx-1_3	19.25	3.91	0.38	1.02	15.72
wago-9(IP)_wt_1	37.31	1.37	0.10	0.18	25.97
wago-9(IP)_wt_2	18.12	1.11	0.05	0.15	27.45
wago-9(IP)_wt_3	16.44	1.31	0.08	0.22	28.08
wago-9(IP)_znfx-1_1	29.08	1.12	0.10	0.21	30.62
wago-9(IP)_znfx-1_2	23.62	1.15	0.06	0.37	33.57
wago-9(IP)_znfx-1_3	17.98	0.81	0.04	0.17	32.32

Total read is in millions.

Supplementary Table 3. Related to Figure 6. % of genes up or down in 22G targeting in znfx-1 mutant at 5' or 3' 10% of the gene.

	up in znfx	down in znfx	total genes	up %	down %
csr 5'	173	9	606	28.55	1.49
wago 5'	366	39	789	46.39	4.94
csr 3'	3	190	606	0.50	31.35
wago 3'	27	354	789	3.42	44.87

Table S4. Cold-sensitive RNAi defect of *znfx-1*(ne4338) is suppressed by *prg-1*. Related to Table 1.

Genotype	*pos-1* food % hatching	L4440 % hatching
Wildtype	0 (4946)	99.7 (1040)
***znfx-1*(ne4338)**	4.6 (4414)	99.6 (1299)
***prg-1*(tm872)**	0 (4034)	93.3 (907)
***prg-1*(tm872)** ***znfx-1*(ne4338)**	0 (3833)	94.7 (883)

% of eggs hatching are shown. Numbers in parentheses indicate the numbers of eggs scored.